Calculation of NMR line shapes in calcium fluoride from modified moment expansions

G. W. Parker and F. Lado
Department of Physics, North Carolina State University, Raleigh, North Carolina 27607
(Received 23 July 1973)

Theoretical second, fourth, sixth, and eighth moments of nuclear-magnetic-resonance absorption lines in calcium fluoride are used to examine the convergence of two different modified moment expansions for free-induction-decay (fid) curves. These expansions provide a systematic method of obtaining corrections to two initial approximations to a line shape which are obtained from either the local-field model, which gives a Gaussian fid curve, or the Abragam function. In the former case one obtains the Fourier transform of the Gram-Charlier expansion and in the latter case a Neumann expansion. These expansions may also be applied to the memory function, a local-field correlation function, rather than the fid function since, in general, the functional form of a memory function is insensitive to the form of a line shape and, in particular, these two curves are similar in shape for dipolar-broadened resonance lines. In analyzing the results of these expansions we are led to formulate a condition for oscillations in an fid curve. This condition is that local-field correlations persist for a time T_2^{**} which is at least of the order of the mean beat period $M_2^{-1/2}$. Here M_2 is the second moment of the resonance line and T_2^{**} is the relaxation time of the memory function. Also, a new trial function is proposed for CaF_2 fid curves which gives the proper behavior at both long and short times.

I. INTRODUCTION

The moments of an NMR absorption line completely determine its shape and that of its associated free-induction-decay (fid) curve. At least the first few of these moments may be calculated exactly, as shown by Van Vleck,[1] who evaluated the second and fourth moments for a rigid-lattice spin system with dipole-dipole and exchange interactions. Recently the sixth[2,3] and eighth[3] moments have been determined for a similar system limited to dipolar interactions between spins. These results apply to the F^{19} spins in calcium fluoride, a system for which extensive experimental results are available.[4-6] It is therefore of interest to compare this data with theoretical line shapes obtained using these moments. This kind of approach represents a compromise between a qualitative description and full calculation of the relevant spin autocorrelation function and it utilizes a qualitative form of an absorption line or fid curve as an initial approximation together with some lower-order moments, which are used to correct and improve this initial shape.

For example, an approach to the line-shape problem in calcium fluoride may be based on the local-field model of dipolar broadening[7] which is applicable to this spin system. Describing the dipole-dipole interaction by a local field along the external field, thus neglecting the spin "flip-flop" terms in the Hamiltonian, one obtains essentially a Gaussian line shape and therefore a Gaussian fid curve. This prediction is in rough qualitative and quantitative agreement with experiment and a systematic method of obtaining correction terms is available. This method is based on the Gram-Charlier expansion.[8-10]

The Gram-Charlier expansion, or more precisely its Fourier transform, is an example of a reformulation or reorganization of the basic moment expansion for an fid curve. The moment expansion of a normalized fid curve is[11]

$$G(t) = G(0)(1 - M_2 t^2/2! + M_4 t^4/4! - \cdots)$$
$$= G(0)\sum_{n=0}^{\infty}(-1)^n M_{2n} t^{2n}/(2n)!, \qquad (1)$$
$$G(0) = 1.$$

The moments M_{2n} are defined by

$$M_{2n} = \int_0^\infty \omega^{2n}\tilde{G}(\omega)\,d\omega\ ,$$
$$\int_0^\infty \tilde{G}(\omega)\,d\omega = 1\ ,$$

where $\tilde{G}(\omega)$ is a normalized line-shape function assumed symmetric about $\omega = 0$. The moment expansion (1) applies to all symmetric line shapes. In order to obtain an expansion reflecting the approximant Gaussian shape of a CaF_2 fid curve one writes $G(t) = e^{-\alpha^2 t^2} g(t)$, where $g(t)$ is determined by (1) and the choice of α. This modified moment expansion has the form

$$G(t) = e^{-\alpha^2 t^2}\sum_{n=0}^{\infty}(-1)^n a_{2n} t^{2n}/(2n)!\ , \qquad (2)$$
$$a_0 = 1\ .$$

Choosing α so that the Gaussian approximation has the correct second moment gives

$$\alpha^2 = \tfrac{1}{2}M_2,\quad a_2 = 0\ ,$$
$$a_4 = M_2^2(M_4/M_2^2 - 3)\ ,$$
$$a_6 = M_2^3(M_4/M_2^3 - 15M_4/M_2^2 + 30)\ ,$$

$$a_8 = M_2^4(M_8/M_2^4 - 28M_6/M_2^3 + 210M_4/M_2^2 - 315) . \quad (3)$$

If a line-shape was precisely Gaussian then its associated fid curve would be $e^{-(M_2t^2/2)}$ and all but the first of the coefficients a_{2n} would vanish. Thus, for this choice of α, the terms in (2) are corrections for a non-Gaussian line shape.

A different modified moment expansion may be obtained as a Neumann expansion involving Bessel functions.[9] The development of this expansion was originally motivated in part by the behavior of terms in an fid expansion based on the basic formula[11]

$$G(t) = \mathrm{Tr}\{S_x(t)S_x\}/\mathrm{Tr}\{S_x^2\} . \quad (4)$$

A particular operator expansion technique for the evaluation of (4) gives a series of functions, successive terms of which have the appearance of Bessel functions of successively higher order multiplied by some function which decays monotonically to zero.[12] Now it has been shown by Abragam[13] that the particular function

$$G_A(t) = e^{-\alpha^2 t^2}\sin(\beta t)/\beta t$$

gives a good description of fid curves in CaF_2 when α and β are determined by the requirement that G_A give the correct M_2 and M_4. A systematic method for obtaining correction terms to G_A could then be based on the Neumann expansion[9]

$$G(t) = e^{-\alpha^2 t^2}\sum_{n=0}^{\infty} b_{2n} J_{2n+\nu}(\beta t)/(\beta t)^{\nu} , \quad (5)$$

where $\nu \neq -1, -2, -3, \cdots$, the J_μ are Bessel functions of order μ, and the coefficients b_{2n} are determined by moments through M_{2n} and the choice of α and β. The optimum leading term is obtained when ν is chosen so that the correct pattern of zeros of G is obtained. From CaF_2 fid data it is found that $G = 0$ when $t \cong t_1, 2t_1, 3t_1, \ldots$, where t_1 is the time from the beginning of a decay to the first zero. This pattern of zeros is reproduced by choosing $\nu = \frac{1}{2}$. If, in addition, α and β are chosen so that the first term gives the correct M_2 and M_4 then (5) becomes

$$\begin{aligned} G(t) &= G_A(t) + e^{-\alpha^2 t^2}\sum_{n=3}^{\infty} c_{2n} j_{2n}(\beta t) , \\ \alpha^2 &= \tfrac{1}{2}M_2\{1 - [\tfrac{5}{6}(3 - M_4/M_2^2)]^{1/2}\} , \\ \beta^2 &= M_2[\tfrac{15}{2}(3 - M_4/M_2^2)]^{1/2} . \end{aligned} \quad (6)$$

In this expansion $c_{2n} = (2/\pi)^{1/2} b_{2n}$ and the j_{2n} are spherical Bessel functions. Explicit expressions for the coefficients c_6 and c_8 are rather lengthy and can be obtained from results given elsewhere.[9]

Another approach to the calculation of line shapes may be based on a formal solution of the line-shape problem which relates an fid curve $G(t)$ to a certain auxiliary function $K(t)$, the memory function. This relation is

$$\frac{dG(t)}{dt} = -\int_0^t K(t - t')G(t')\,dt' . \quad (7)$$

The memory function thus relates the rate of change of G at one time to its values at earlier times, and its Laplace transform may be expressed as the ratio of two infinite-order determinants involving the moments of the absorption line.[14] Furthermore, it may be shown to behave in the fashion of a local-field correlation function.[15] For example, $K(t)$ decays to zero from its initial value $K(0)$ in a time of the order of T_2^{**} which varies widely according to the character of the spin-lattice system. In rigid-lattice solids, like CaF_2, $T_2^{**} \approx M_2^{-1/2}$, whereas in nonviscous liquids $T_2^{**} \ll M_2^{-1/2}$. Since in CaF_2 the decay of $G(t)$ occurs in a time $T_2^{*} \approx M_2^{-1/2}$,[16] $G(t)$ and $K(t)$ both decay in about the same time and, in fact, they are similar in shape.[15] This suggests that we calculate an fid curve indirectly using (7) by applying the modified moment expansions to $K(t)$. Further motivation for this approach is based on the fact that G has been found to be less sensitive to approximations made to K than to similar approximations made directly to G.[14,15]

The moment expansion of $K(t)$ is obtained from (1) and (7) and is

$$\begin{aligned} K(t) &= K(0)(1 - M_2't^2/2! + M_4't^4/4! - \cdots) \\ &= K(0)\sum_{n=0}^{\infty}(-1)^n M_{2n}' t^n/(2n)! . \end{aligned} \quad (8)$$

The parameters in this expansion are

$$\begin{aligned} &K(0) = M_2, \quad M_2' = M_2(M_4/M_2^2 - 1) , \\ &M_4' = M_2^2(M_6/M_2^3 - 2M_4/M_2^2 + 1) , \\ &M_6' = M_2^3[M_8/M_2^4 - 2M_6/M_2^3 \\ &\qquad + (3 - M_4/M_2^2)M_4/M_2^2 - 1] . \end{aligned} \quad (9)$$

We obtain modified moment expansions of the form (2) and (6) by using (8) and (9) with M_{2n}' and $K(0)$ used in place of M_{2n} and $G(0)$. The calculations of G from K presented in Sec. II were performed by a method based on (7) which has been described previously.[15]

II. RESULTS

Theoretical moments for CaF_2[3,17] expressed as ratios to the second moment are given in Table I, where they are compared to moment ratios for a Gaussian and a rectangular line shape. These comparisons show that the calcium fluoride line shapes are more nearly rectangular than Gaussian and that the actual moment ratios are less than the Gaussian moment ratios, i.e., $M_{2n}/(M_2)^n \leq (2n)!/$

TABLE I. Theoretical moments for calcium fluoride [G. W. Canters and C. S. Johnson, Jr., J. Mag. Res. 6, 1 (1972); S. J. K. Jensen and E. K. Hansen, Phys. Rev. B 7, 2910 (1973)] compared to moments of Gaussian and rectangular line shapes.

	CaF_2			
	[100]	[111]	Gaussian	Rectangular
$M_2^{1/2}$ (G)	3.570	1.480	•••	•••
$M_2^{-1/2}$ (μsec)	11.13	26.85	•••	•••
M_4/M_2^2	2.125	2.373	3	1.8
M_6/M_2^3	6.325	8.485	15	3.9
M_8/M_2^4	25.14	43.75	105	9.0

$(2^n n!)$ for $n \leq 4$. Assuming this inequality to hold for all n, it follows by comparison with the Gaussian fid curve that the moment expansion (1) is uniformly convergent for $0 \leq t < \infty$. Consequently, the modified moment expansions have the same property.[9] Their rate of convergence for a specified interval of time may be determined by comparison with experiment.

In Figs. 1(a) and 1(b) the moment expansion (1) truncated after the M_8 term and the Abragam function are compared to the data of Barnaal and Lowe (BL)[5] for two principal crystal orientations. The truncated moment expansion is accurate for $t \lesssim \frac{3}{2} \times M_2^{-1/2}$ and it ultimately diverges. The Abragam function gives good agreement with the data through the second zero but it decays too rapidly thereafter, as shown in Fig. 1(a).

As an alternative to the moment expansion one could calculate upper and lower bounds to $G(t)$. However, bounds based on moments through M_8 would become well separated in the neighborhood of the first minimum of G, according to results of applications to other similar line shapes.[18]

The expansion (6) may be used to calculate corrections to G_A using M_6 and M_8 to evaluate c_6 and c_8. We will label any correction term depending on M_6 and lower moments, G_1, or first order. Terms depending on M_8 and lower-order moments will be labeled G_2, or second order, while G_0 is a zeroth-order term depending on M_4 and M_2. For the expansion (6) $G_0 = G_A$. G_1 and G_2 obtained from (6) for [100] orientation are shown in Fig. 2. Results for [111] orientation are similar in form. These terms are of opposite sign and initially zero. G_2 increases more rapidly than $|G_1|$, however, so that for this initial period of time $G_1 + G_2$ is positive, thus tending to improve agreement of the truncated expansion with the data of BL. However, it is evident from the numerical values of G_1 and G_2 that more terms are needed in the series for this range of t. A disadvantage of pursuing this approach that emerges from numerical application of (6) is that the coefficients are quite sensitive functions of the moments. For example, changing M_8 by 1% causes c_8 to change by about 14%.[19] This feature of the Neumann expansion (6) is not a property of the Gram-Charlier expansion (2).

In Figs. 3(a) and 3(b) is shown the zeroth-, first-, and second-order approximations to G calculated from the Gram-Charlier expansion for [100] and [111] orientations. For the moments given in Table I the coefficients a_6 and a_8 have opposite signs so that G_1 and G_2 are both negative for $t > 0$, as can be seen in these figures. The second-order approximation is in good agreement with the data through the first minimum but the truncated expansion cannot subsequently become positive so that oscillations are not obtained. Applying the same type of expansion to the memory function,

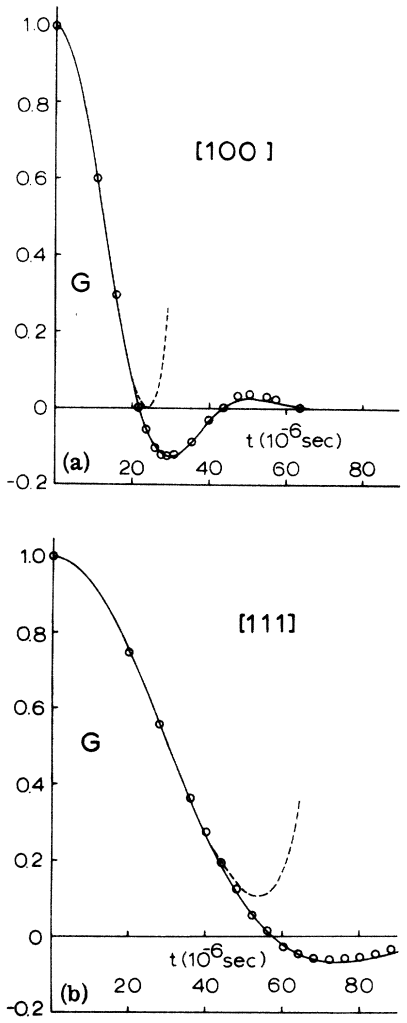

FIG. 1. (a) Abragam function (solid curve) and truncated-moment expansion (dashed curve) compared to experimental data of Barnaal and Lowe (circles) for [100] orientation. Units of time are microseconds. (b) The same comparisons as in (a) for [111] orientation.

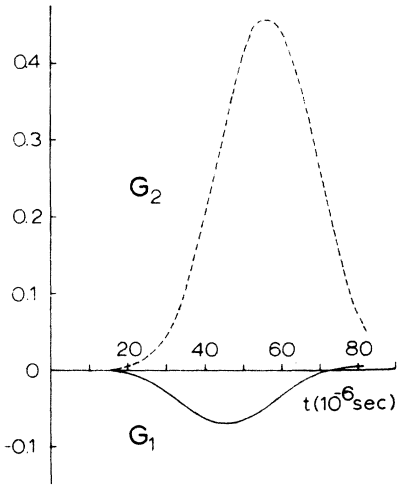

FIG. 2. First-order (dashed curve) and second-order (solid curve) correction terms in the $\nu=\frac{1}{2}$ Neumann expansion for [100] orientation. Units of time are microseconds.

however, gives the results shown in Figs. 4(a) and 4(b). In particular, by comparing Fig. 3(a) and Fig. 4(a) it is seen that convergence is better in the latter figure since oscillations of about the correct period and amplitude are obtained in the second-order approximation. In fact, each order of approximation to K produces an oscillatory fid curve. The period of oscillation approaches that of the experimental data as more terms are included in the memory-function expansion. These oscillations are found to occur with the same periodicity in the long-time form of a calcium fluoride fid curve.

For $t \gtrsim 5M_2^{-1/2}$ the calculated fid curves in Fig. 4 are described by the equation

$$G(t) \cong de^{-at}\cos(bt+c) .$$

This form has been found to be characteristic of CaF_2 fid curves at long times[15,20] and it is revealed by a plot of $\ln|G_p|$, where G_p is the value of G at its peaks, as a function of the time of occurrence of these peaks. The slope of the resulting straight line gives the parameter a. The parameter b is obtained from the periodicity of the zeros of G. Values of these parameters obtained in this manner from the second-order approximation of Fig. 4 are listed in Table II as a (calc.) and b (calc.) together with the values obtained from the data of Lowe, Bruce, Kessemeier, and Gara (LBKG).[6,15] Comparison of these values shows that the second-order fid curves of Fig. 4 decay too rapidly to zero at longer times since a (calc.) $>a$ (expt.). The other orders of approximation give nearly the same value of a (calc.) but different values of b (calc.), as shown in Fig. 4. Since the period of oscillation of a given CaF_2 fid curve is found to be the same at both long and short times it is appropriate to obtain this value from the data of BL. This additional data has been included in the last column of Table II. For the [111] orientation there is a discrepancy between the data of BL and that of LBKG. This may be due to the crystal used by BL being aligned better than that of LBKG.[5]

Line shapes obtained from the zeroth- and second-order Gram-Charlier memory-function expansion for [100] orientation are compared with the data of Bruce in Fig. 5. All three line shapes are normalized to the same area. The zeroth-order approximation corresponds to a Gaussian memory function which depends on M_2 and M_4 as shown by (8) and (9), and it resembles a broadened pair line shape.[15] The first- and second-order corrections improve the line shape, particularly near the center of the line. This corresponds to improvement in the long-time behavior of the associated fid curve.

III. DISCUSSION

The existence of oscillations in an fid curve may be related to the value of T_2^{**}, the relaxation time

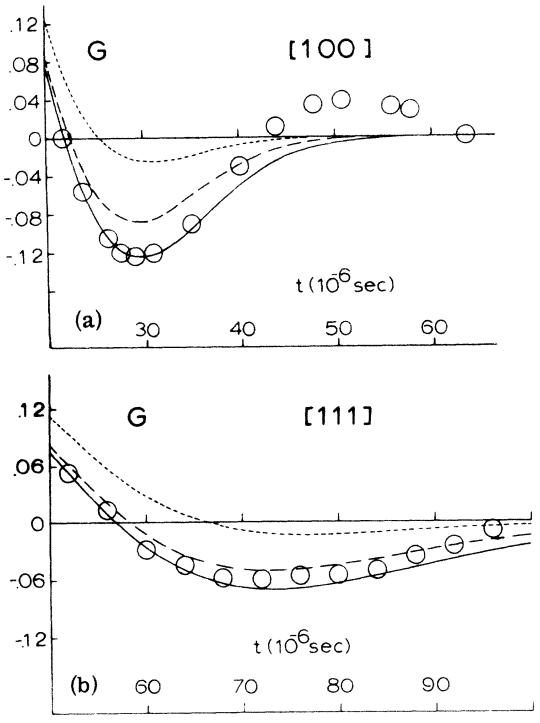

FIG. 3. (a) Zeroth-order (small dashed curve), first-order (large dashed curve), and second-order (solid curve) Gram-Charlier approximations to [100] fid curve compared to the data of Barnaal and Lowe (circles). Units of time are microseconds. (b) The same comparisons as in (a) for [111] orientation.

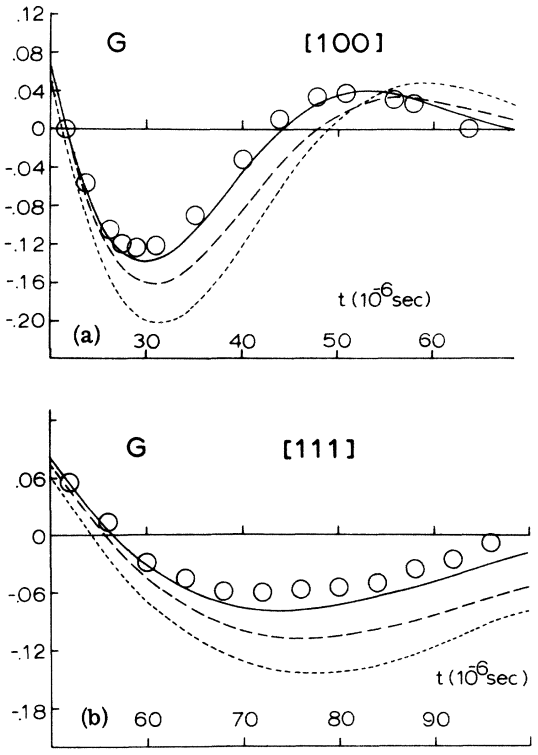

FIG. 4. (a) Zeroth-order (small dashed curve), first-order (large dashed curve), and second-order (solid curve) approximations to [100] fid curve obtained from zeroth-, first-, and second-order Gram-Charlier approximations to memory function. Comparison is made with the data of Barnaal and Lowe (circles). Units of time are microseconds. (b) The same comparisons as in (a) for [111] orientation.

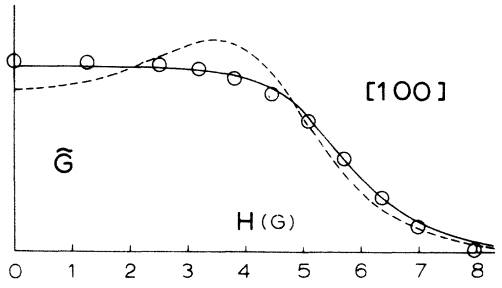

FIG. 5. Zeroth-order (dashed curve) and second-order (solid curve) absorption line shapes for [100] orientation obtained by Fourier transformation of the zeroth- and second-order fid curves of Fig. 4(a). Comparison is made to data of Bruce (circles) by normalizing all three line shapes to the same area. Units of magnetic field are gauss.

of the local-field correlation function $K(t)$. We recall that $M_2^{1/2}$ gives the average beat frequency in a spin system which is unchanged by lattice motions and spin exchange. If there were only very slow fluctuations in the local field, i.e., $T_2^{**} \gg M_2^{-1/2}$, then an fid curve would exhibit oscillations at a frequency $\omega \approx M_2^{1/2}$. In this limit the motion of an individual spin in a frame of reference rotating at the Larmor frequency would be precessional in character since the average beat period is much less than the time required for a significant change in local field. If, however, the fluctuations were rapid so that $T_2^{**} \ll M_2^{-1/2}$, then individual spin motion in the rotating frame would be of the random-walk type[21] and the fid curve would be nonoscillatory. The condition for oscillations in an fid curve is then that local-field correlations persist for a time greater than or of the order of the average beat period, i.e., $T_2^{**} \gtrsim M_2^{-1/2}$.

The validity of this inequality may be illustrated by considering a hypothetical spin system consisting of a large number of identical spin-$\frac{1}{2}$ particles subject to variations in spatial density and temperature which allow the fourth-moment ratio of their resonance line to vary between one and infinity. Three limiting cases may be distinguished. These situations have been described in an earlier publication in which they were characterized by their relative values of T_2^*, T_2^{**}, and $M_2^{-1/2}$.[15] First, if these spins are arranged uniformly in pairs, each pair having the same orientation with respect to the external field, then their resonance line would approach a pair of δ functions at $\omega = \pm M_2^{1/2}$ as the distance between pairs is increased.[22] This is the *pair limit* in which $T_2^* > T_2^{**} \gg M_2^{-1/2}$ and $M_4/M_2^2 \to 1$. Second, bringing spin pairs together produces a broadening of the pair spectrum and ultimately, in the *solid limit*, a single broad line corresponding to a more or less uniform distribution of spins. This limit is characterized by the relations $T_2^* \approx T_2^{**} \approx M_2^{-1/2}$. Third, if lattice motion is introduced the resonance line is narrowed to Lorentzian form as $M_4/M_2^2 \to \infty$. This is the *Lorentzian limit*, for which $T_2^* \gg M_2^{-1/2} \gg T_2^{**}$.

TABLE II. Parameters in long-time form of calcium fluoride fid curves.

Orientation	a (calc.) (μsec^{-1})	a (expt.) (μsec^{-1})	π/b (calc.) (μsec)	π/b (expt.) (μsec)	π/b (expt., BL) (μsec)
[100]	0.059	0.037	23.8	21.5	21.6
[111]	0.031	0.022	57	44	57

The local-field correlation function's relaxation time T_2^{**} decreases in this succession of line shapes in contrast to the transverse relaxation time T_2^*, which decreases to a minimum of the order of $M_2^{-1/2}$ and then increases during motional narrowing. This behavior of T_2^{**} is consistent with its interpretation as the decay time of a local-field correlation function.[15]

We may use the succession of line shapes just described to examine the possibility of oscillations in an fid curve. The relation between $G(t)$ and $\tilde{G}(\omega)$ is given by[11]

$$G(t)=\int_0^\infty \tilde{G}(\omega)\cos(\omega t)\,d\omega \ .$$

We look for the time t_1 for which $G(t)$ first becomes negative.[23] Now $\tilde{G}(\omega)$ is positive for $-\infty < \omega < \infty$ and its values are significant only for those frequencies for which $|\omega| \lesssim M_2^{1/2}$. Therefore, for some time t_1 appreciably greater than $\pi/M_2^{1/2}$ the overlap between $\tilde{G}$ and $\cos(\omega t_1)$ will necessarily produce a positive value of $G(t_1)$. For $t \approx \pi/M_2^{1/2}$, however, the range of frequencies for which $\cos(\pi\omega/M_2^{1/2})$ first becomes negative will overlap the region where $\tilde{G}$ is significant, thus allowing $G(t_1)$ to become negative. In the pair limit and for some broadened pair lines we have the bulk of $\tilde{G}$ in the negative region of $\cos(\pi\omega/M_2^{1/2})$. Fid curves for these line shapes oscillate at frequencies near $M_2^{1/2}$. Line shapes giving more weight to frequencies near zero than broadened pair line shapes will require a smaller value of t_1 to make $G(t_1)$ negative, if, indeed, it is possible at all. In the solid limit one is approaching the transition to a nonoscillatory fid curve. For example, a Gaussian line shape having $M_4/M_2^2 \approx 3$ produces a Gaussian fid curve, whereas the more flat-topped line shapes found in CaF_2 have $M_4/M_2^2 \approx 2$ and their fid curves oscillate at frequencies of the order of $M_2^{1/2}$ (Fig. 1). During the transition from a Gaussian-like line to a Lorentzian line increasing weight is given to frequencies near zero, there are no oscillations in the associated fid curves, and one has $T_2^{**} < M_2^{-1/2}$. In the transition from the pair limit to the solid limit, however, fid curves exhibit oscillations which become increasingly damped as the solid limit is approached and $T_2^{**} \lesssim M_2^{-1/2}$.

To summarize, the succession of simple line shapes just described shows that the existence of oscillations in an fid curve is consistent with the condition $T_2^{**} \gtrsim M_2^{-1/2}$. They also seem to imply that an equivalent condition is $M_4/M_2^2 \lesssim 3$, but this is not true, in general, since more complex lineshapes, consisting of several component lines, may have $M_4/M_2^2 \approx 3$ and $T_2^{**} \gg M_2^{-1/2}$.

A trial function exhibiting some of the behavior just described is

$$G_T(t)=\alpha t\,\mathrm{csch}(\alpha t)\sin(\beta t)/\beta t \ ,$$
$$\alpha^2=\tfrac{1}{4}M_2(5M_4/M_2^2-9) \ ,$$
$$\beta^2=\tfrac{1}{4}M_2(21-5M_4/M_2^2) \ . \qquad (10)$$

These values of α and β are chosen so that G_T gives the correct second and fourth moments. The function G_T is meaningful as an fid curve only for real values of α, which requires $M_4/M_2^2 \geq 9/5$. When $M_4/M_2^2 = 9/5$ we obtain the fid curve associated with a rectangular line shape which is nonzero for $|\omega| \leq \beta$. For somewhat larger values of M_4/M_2^2 damped oscillations are obtained whose frequency β remains approximately equal to $M_2^{1/2}$ except in the neighborhood of the transition point at $M_4/M_2^2 = 21/5$, where these oscillations have such small amplitudes ($\alpha/\beta \gg 1$) that they would be unobservable. The range $9/5 \leq M_4/M_2^2 < 21/5$ includes values of the fourth-moment ratios in CaF_2. In fact, G_T gives a good description of CaF_2 fid curves at both long and short times. For example, using values of α and β determined by theoretical values of M_2 and M_4 we may obtain values for the higher moments from (10). For [100] orientation these predicted moment ratios are $M_6/M_2^3 = 6.27$ and $M_8/M_2^4 = 22.8$, while for [111] orientation one finds that $M_6/M_2^3 = 8.71$ and $M_8/M_2^4 = 45.6$. These ratios are quite close to those given in Table I. When compared to the Abragam function shown in Fig. 1, G_T is found to give oscillations having slightly greater amplitudes. The half-periods of these oscillations are given in Table III and are in good agreement with experiment. The long-time form of G_T is

$$G_T \to (\alpha/\beta)\sin(\beta t)e^{-\alpha t} \quad \text{for } t \gg M_2^{-1/2}. \qquad (11)$$

The values of α in (11) are given in Table III. They are nearly equal to those given in Table II for a (calc.). Consequently, the function G_T gives a better description of the observed fid curves than either the Abragam function or the truncated expansions previously described. On the other side of the transition point at $M_4/M_2^2 = 21/5$, β^2 becomes negative so that G_T may be written as $\alpha\sinh(\alpha t)/\gamma\sinh(\gamma t)$, where $i\gamma = \beta$. Now, for large values of M_4/M_2^2 G_T approaches the correct limit; i.e., as $M_4/M_2^2 \to \infty$ we obtain

$$G_T \to e^{-t/T_2} \quad \text{for } t \gtrsim M_2^{-1/2} \ .$$

TABLE III. Parameter values in trial function applied to calcium fluoride.

Orientation	α (μsec^{-1})	π/β (μsec)
[100]	0.057	21.7
[111]	0.032	55.8

The relaxation time is given by

$$\frac{1}{T_2} \approx \frac{3}{\sqrt{5}} \frac{M_2^{3/2}}{M_4^{1/2}} .$$

This expression for T_2 is in accord with the usual estimates of this quantity that are based on the values of M_2 and M_4.[13]

The normalized line shape corresponding to (10) is given by

$$\tilde{G}_T(\omega) = \frac{(2\beta)^{-1} \sinh(\pi\beta/\alpha)}{\cosh(\pi\omega/\alpha) + \cosh(\pi\beta/\alpha)} . \tag{12}$$

This transform is valid for $M_4/M_2^2 \geq 9/5$. For $|\omega| \ll \alpha$ a Lorentzian form is obtained from (12). When, in addition, $M_4/M_2^2 \gg 1$, this Lorentzian form is valid for $|\omega| \lesssim M_2^{1/2}$. In the wings of this line, however, where $|\omega| \gg \alpha$, $\tilde{G}_T$ has an exponentially decaying form.

[1]J. H. Van Vleck, Phys. Rev. 74, 1148 (1948).

[2]E. T. Cheng and J. D. Memory, Phys. Rev. B 6, 1714 (1972); W. F. Wurzbach and S. Gade, Phys. Rev. B 6, 1724 (1972); W. F. Wurzbach, S. Gade, E. T. Cheng, and J. D. Memory, Phys. Rev. B 7, 2209 (1973).

[3]S. J. K. Jensen and E. K. Hansen, Phys. Rev. B 7, 2910 (1973).

[4]C. R. Bruce, Phys. Rev. 107, 43 (1957).

[5]D. E. Barnaal and I. J. Lowe, Phys. Rev. 148, 328 (1966).

[6]Unpublished data of Lowe, Bruce, Kessemeier, and Gara made available to us by Professor R. E. Norberg.

[7]N. Bloembergen, E. M. Purcell, and R. V. Pound, Phys. Rev. 73, 679 (1948).

[8]H. Cramer, *Mathematical Methods of Statistics* (Princeton U. P., Princeton, N. J., 1945), pp. 222 and 223.

[9]G. W. Parker, Phys. Rev. B 2, 2453 (1970).

[10]B. T. Gravely and J. D. Memory, Phys. Rev. B 3, 3426 (1971).

[11]I. J. Lowe and R. E. Norberg, Phys. Rev. 107, 46 (1957).

[12]H. Betsuyaki, Phys. Rev. Lett. 24, 934 (1970).

[13]A. Abragam, *The Principles of Nuclear Magnetism* (Oxford U. P., London, 1961), Chap. 4.

[14]F. Lado, J. D. Memory, and G. W. Parker, Phys. Rev. B 4, 1406 (1971). A review of different approaches to the line-shape problem may be found in this paper.

[15]G. W. Parker and F. Lado. Phys. Rev. B 8, 3081 (1973).

[16]We are using the same notation as Ref. 15. T_2^* is the relaxation time of the transverse magnetization and T_2^{**} is the relaxation time of the associated local-field correlation function. When the Bloch equations hold exponential decay obtains and $T_2^* = T_2$.

[17]G. W. Canters and C. S. Johnson, Jr., J. Mag. Res. 6, 1 (1972).

[18]O. Platz and R. G. Gordon, Phys. Rev. B 7, 4764 (1973).

[19]In an earlier calculation, Ref. 9, experimental sixth and eighth moments obtained from Bruce's data were used to calculate G_1 and G_2. For these moments these two correction terms practically canceled each other over the initial portion of an fid curve.

[20]P. Borckmans and D. Walgraef, Phys. Rev. Lett. 21, 1516 (1968); Phys. Rev. 167, 282 (1968).

[21]D. Pines and C. P. Slichter, Phys. Rev. 100, 1014 (1955).

[22]G. E. Pake, J. Chem. Phys. 16, 327 (1948).

[23]This restricted condition for oscillations is sufficient here. More complex line shapes give oscillating fid curves which are positive and for which $T_2^{**} \gg M_2^{-1/2}$.